

Scanning tunneling microscopy and spectroscopy of S on Pd(111)

S. Speller, T. Rauch, A. Postnikov, and W. Heiland
Universität Osnabrück, 49069 Osnabrück, Germany
 (Received 24 September 1999)

On the Pd(111) surface ($\sqrt{7} \times \sqrt{7}$) $R19.1^\circ$ S structure was observed. This structure was studied by scanning tunneling microscopy and scanning tunneling spectroscopy (STS). In both modes atomic resolution is achieved. With STS two S species, in fcc and hcp sites of the Pd(111) surface, are identified. Theoretical estimates of the surface density of states show small differences for the S at the two different sites.

INTRODUCTION

Scanning tunneling microscopy (STM) has become a widely used tool in surface science. In comparison scanning tunneling spectroscopy (STS) is used much less frequently, even though the technique holds great promise for the exploration of the local electronic structure of surfaces. For our system, S on Pd, there are several published reports of using STM and low-energy electron diffraction (LEED),¹⁻⁴ some more using LEED only,⁵⁻⁷ and one extended x-ray-absorption fine structures study.⁸ We know of one theoretical paper only describing STS of Pd(111).⁹ Neither the clean surface nor the Pd/S surface have been studied experimentally by STS before, to the best of our knowledge. S on Pd forms several structures identified in the LEED nomenclature as ($\sqrt{3} \times \sqrt{3}$) $R30^\circ$ and ($\sqrt{7} \times \sqrt{7}$) $R19.1^\circ$.¹⁻⁹ STM measurements show that the ($\sqrt{3} \times \sqrt{3}$) $R30^\circ$ structure is not a pure phase on Pd(111) but coexists with disordered structures, (2×2) stripes, and the ($\sqrt{7} \times \sqrt{7}$) $R19.1^\circ$ structure.⁴ The ($\sqrt{7} \times \sqrt{7}$) $R19.1^\circ$ structure, however, can be prepared such that it covers more than 90% of the surface. The rest is disordered S on the surface. In the present paper we report STM/STS results of the ($\sqrt{7} \times \sqrt{7}$) $R19.1^\circ$ surface. The

problem with the ($\sqrt{7} \times \sqrt{7}$) $R19.1^\circ$ S surface is that there exist three different structure models, in part due to differences of the S coverage which range from 1/7 of a monolayer,³ 2/7 of a monolayer,⁴ to 3/7 of a monolayer.^{1,5-8} Hence the number of S atoms in the unit cell of the ($\sqrt{7} \times \sqrt{7}$) $R19.1^\circ$ S structure is under discussion. This problem is then related to the question of what is seen in STM topographs. There is good evidence that bumps on S-covered surfaces are due to the adsorbed S atoms,¹⁰ but in the case of the ($\sqrt{7} \times \sqrt{7}$) $R19.1^\circ$ S structure several bumps are seen of different apparent height.⁴ Here we show that with STS the S sites can be positively identified in comparison with the Pd sites.

EXPERIMENT

The experimental procedures to produce the S on Pd structures have been presented in detail before.^{3,4} The Pd(111) surface is cleaned by the usual sequence of sputter and annealing cycles. The main impurity observed by Auger electron spectroscopy (AES) was S segregating to the surface.³ The STM we use is a standard ultra-high-vacuum (UHV) Omicron system. Additional methods are low-energy

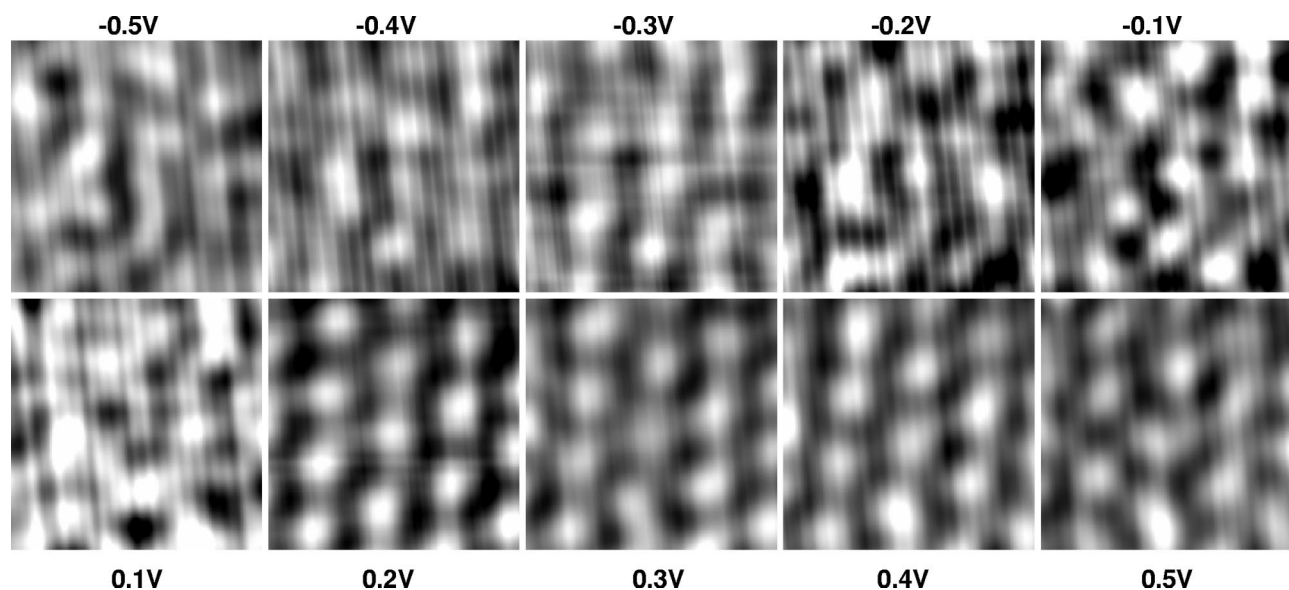


FIG. 1. STS on the clean Pd(111) surface. I maps of a ($9 \text{ \AA} \times 9 \text{ \AA}$) area at varying voltages are shown. The gray scale was applied independently on each image in order to obtain optimal contrast.

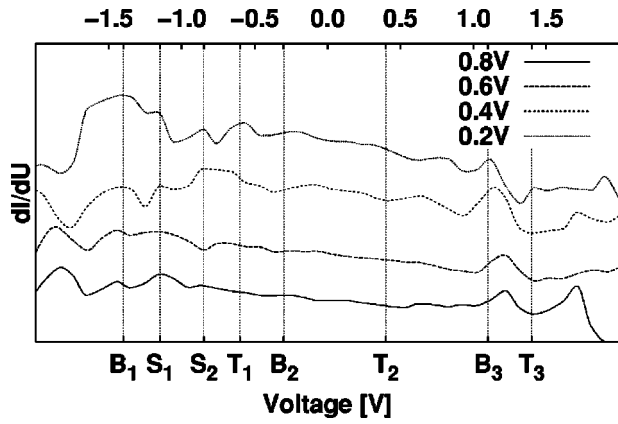


FIG. 2. ST spectra measured on clean Pd(111). At the marked voltages $B_{1,2,3}$ exist enhanced electronic densities of states in the bulk band structure, at the positions $S_{1,2}$ surface states are present, and at $T_{1,2,3}$ maxima are expected by Drakova and Doyen due to the tunnel tip (Ref. 9).

electron diffraction (LEED), reflection high-energy electron diffraction, Auger electron spectroscopy (AES), and x-ray photoelectron spectroscopy (XPS). The S is brought to the surface using H_2S gas. The STM/STS tips are electrochemically etched tungsten tips which are further prepared *in situ* by Ar sputtering and annealing.

RESULTS AND DISCUSSION

The clean Pd(111) surface is presented in Fig. 1 in a sequence of atomically resolved STS images for bias voltages (U) ranging from -0.5 V to 0.5 V. For each frame the voltage and the distance between tip and surface are kept constant. The voltage is applied to the sample. The contrast in the images corresponds to the current measured in each point. The STS images are taken with 50×50 points and 61 spectroscopy data points creating a file of 610 KB. These

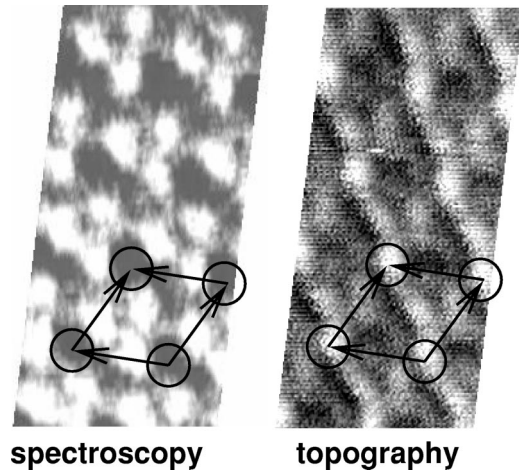


FIG. 3. Comparison of STS and STM images, $15 \text{ \AA} \times 30 \text{ \AA}$, -1 V, 0.5 nA. The STS data are shown as $[(dI/dU)I(U)]_{U_0=-0.1 \text{ V}}$ map.

images represent the local electronic density of states if the accepted ansatz of the STS theory is applicable.⁹ Obviously at a positive bias between 0.2 and 0.4 V good topographic-like images of Pd(111) are obtained.

The spectroscopic data in the dI/dU vs U representation are shown in Fig. 2 for four different positive bias voltages. The capital letters B_1 , etc., refer to the theoretical analysis of the dI/dU spectra.⁹ $B_{1,2,3}$ are correlated to increased electronic densities of the bulk band structure, at $S_{1,2}$ exist surface states, and at $T_{1,2,3}$ tip induced states are expected.⁹ The agreement between theory and experiment is satisfactory. The agreement allows the conclusion that our measurements were taken with a clean W tip. After preparing the $(\sqrt{7} \times \sqrt{7}) R19.1^\circ$ structure we took extended AES and XPS measurements yielding $0.28 \pm 0.04\%$ S at the surface corresponding to two S atoms per surface unit cell.⁴ In the segregation experiments we reached one S atom per surface unit

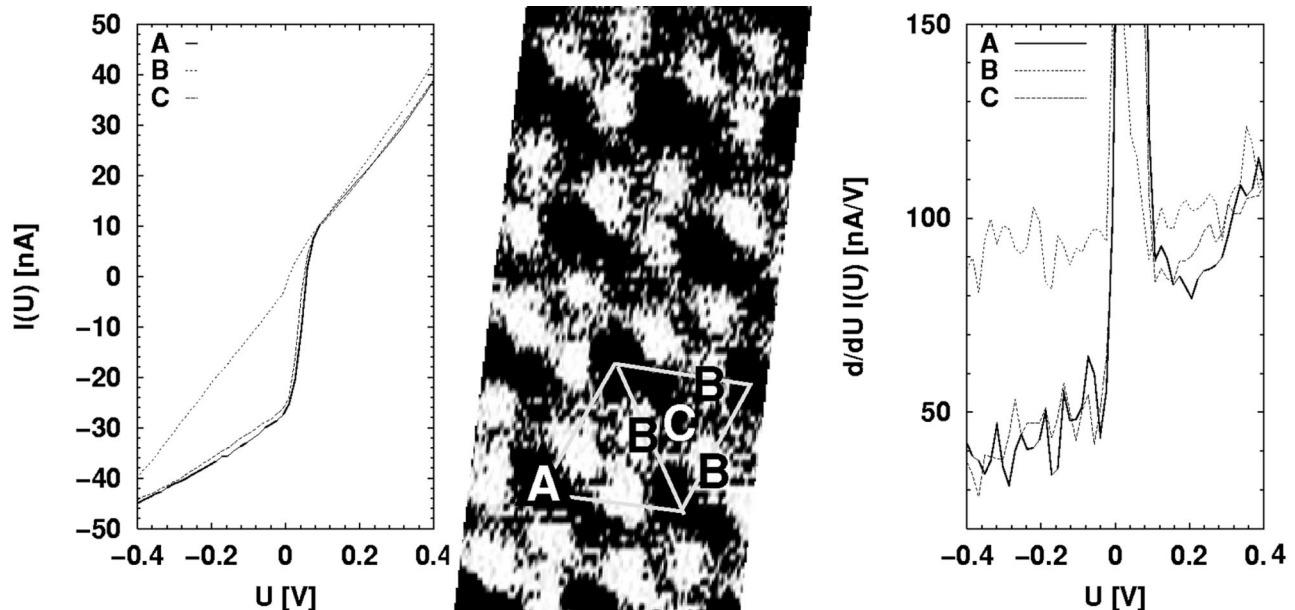


FIG. 4. Atomically resolved STS measurements of the $(\sqrt{7} \times \sqrt{7}) R19.1^\circ$ structure. A, B, C positions refer to S_{fcc} , Pd, and S_{hcp} atoms, respectively. (Left) $I(U)$ curves. (Middle) Drift corrected I image at $U_0 = -0.1$ V. (Right) $(d/dU)I(U)$ curves.

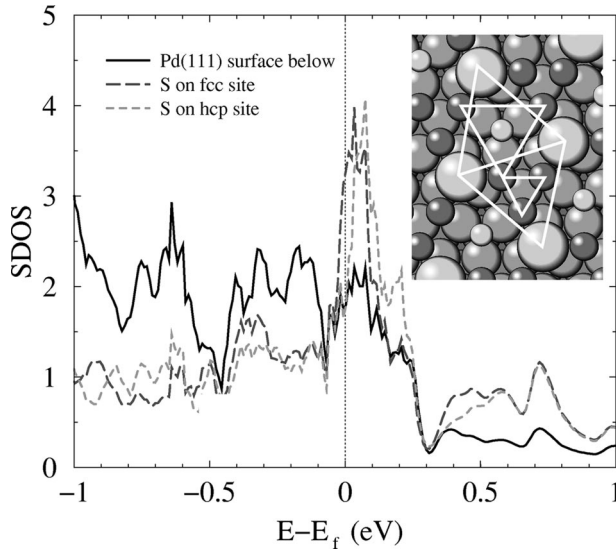


FIG. 5. Density of states per eV for a S atom on a fcc site and an hcp site on Pd(111) (unrelaxed). The inset shows the model of the structure with a mixed layer of two S atoms and three Pd atoms in the unit cell. Light shaded spheres represent S atoms, dark shaded atoms represent Pd atoms in the mixed layer. Light shaded, large spheres are S atoms on fcc sites. Light shaded, and small spheres are S atoms on hcp sites. Dark shaded, small spheres are the Pd atoms of the mixed layer. A unit cell of the hexagonal ($\sqrt{7} \times \sqrt{7}$) $R19.1^\circ$ S structure is marked. In order to distinguish the two halves of this unit cell, the three Pd atoms in the mixed layer are marked in two ways. There are other possible models with two S in the unit cell but the FLAPW calculations support this model (Ref. 4).

cell,³ other groups report three S atoms per unit cell.^{1,5-8} The STM and STS images of the ($\sqrt{7} \times \sqrt{7}$) $R19.1^\circ$ structure are compared in Fig. 3. An obvious conversion of contrast occurs, i.e., the white, elevated bumps of the STM topograph appear dark in the STS constant current image and vice versa. This is especially important for the weaker of the white bumps of the STM image which is difficult to identify as either S or Pd from the STM topograph only. The STS constant current image gives qualitative verification that the small bump is S if the big bump is S. This qualitative information is corroborated by the I vs U and the dI/dU vs U analysis (Fig. 4). We show here an I map at $U = -0.1$ V, which is similar to the STS image of Fig. 3, where the Pd sites B and the S sites A and C are marked, respectively. The S sites deliver a much lower current at negative bias voltage than the Pd sites. Correspondingly the S sites have lower conductivity at negative voltages than the Pd sites. The Pd-tip tunnel contact is clearly Ohmic, whereas the S tip contact is of diode character. At higher positive bias voltages the characteristic curves of the S-tip contact and the Pd-tip contact are identical.

In the naive picture of the surface-tip contact with the negative bias, electrons tunnel from the surface to the tip and vice versa at positive bias. Since there are occupied and empty states below and above the Fermi level available in the band structure of Pd, Ohmic behavior is observed naturally. With S adsorbed on the surface the problem becomes more involved. The electronic state of S will depend in detail on the theoretical model used for determining the bonding site, the bonding energies, the occupied and unoccupied lev-

TABLE I. Occupation of electronic states within small energy intervals below and above E_F inside the atomic sphere at a S site in fcc and hcp positions on Pd(111).

	$(E_F - 0.2 \text{ eV}; E_F)$	$(E_F; E_F + 0.2 \text{ eV})$
fcc	0.29	0.50
hcp	0.26	0.55

els, etc. In most cases S will form a negative entity, S^{2-} like, on a metal surface. S^{2-} like means that the available orbitals are partly filled. E.g., for CuS(001) in the form of covellite the occupations, i.e., the Mulliken charges, have been estimated as -1.428 and -0.711 for trigonal and tetrahedral S ligand sites, respectively.¹¹ The binding energies are of the order of 6–8 eV for CuS and for most other S on a metal system reported (S on W(001), Ref. 12 and references therein). In the naive picture the electrons at the S site would then not be available for tunneling, because they are too much below the Fermi energy, so they appear dark at negative bias and bright at positive bias.

The problem of different STM contrast for different S sites [S on Mo (Ref. 13)], and the dependence of the contrast on the electronegativity has been discussed before.¹⁰ The contrast differences in the case of S on Mo were ascribed to mixing of atomic orbitals, i.e., d Mo with $3p_z$ S, causing interferences in the tunneling channels over different S sites. The analysis of contrasts in STM with respect to the electronegativity is based on a different theoretical approach,¹⁰ but agrees in part with the results of the previously named authors.¹³ From the point of view of the ($\sqrt{7} \times \sqrt{7}$) $R19.1^\circ$ S structure on Pd(111), the two S atoms identified by STS but having different STM contrast could have different electronegativities. Alternatively, the STM contrast can be due to a real space height difference as well. Since in STM topographies the S atom sitting on a fcc site is measured larger and the one sitting on a hcp site is measured smaller, the question arises whether this is an effect from a difference in the electronegativity of the adsorption sites or a true height difference, i.e., a different relaxation of the position of the S atom with respect to the surrounding Pd atoms.

Furthermore, S on a fcc hollow site has three direct Pd neighbors whereas on a hcp site there is one additional direct Pd neighbor at a distance of $1.155a$. Intuitively, a slightly higher electron density may be expected on the hcp site. In Fig. 5 we show the surface density of states (SDOS) for S on Pd(111) for the two sites in question. The calculations are based on the tight-binding approach. There is an obvious shift of the charge distribution between the hcp and fcc site S. When integrating the SDOS from -0.2 eV to 0 eV and from 0 eV to $+0.2$ eV, we obtain information on the charge leading to the tunneling current (Table I).

The charge differences between the two sites are small albeit with a higher charge on the hcp site. The charge difference between the $-$ range and the $+$ range agrees qualitatively with the STS data. The charge on Pd is almost independent of the bias within the ranges chosen, i.e., 0.373 for the $-$ range and 0.358 for the $+$ range, respectively. The lower charge compared to S agrees with the STM topography, the independence of the sign agrees with the STS data. In the SDOS calculations no relaxation of the S atoms

(height correction) or of the Pd lattice is taken into account. On the other hand, full potential linear augmented plane wave (FLAPW) calculations of the $(\sqrt{7} \times \sqrt{7}) R19.1^\circ$ structure yields a shift of three Pd atoms towards the S atom on the hcp site, which will cause the S on this site to be more embedded than the S on the fcc site as shown in the model inset of Fig. 5. These Pd atoms are seen as *B* in the STS image (Fig. 4). So we conclude that the apparent size difference in the STM topography is due to a height difference of the S atom on the fcc and hcp adsorption sites of the Pd(111) surface.

So, for our case we favor the electronegativity model¹⁰ with some corrections for possible real space height differences compared to the tunneling channel model.¹³ The STS results corroborate the 2 S-atom mixed layer model of the $(\sqrt{7} \times \sqrt{7}) R19.1^\circ$ S structure evaluated from STM results and FLAPW calculations cited.

ACKNOWLEDGMENT

This work was supported by the Deutsche Forschungsgemeinschaft (DFG).

¹C. H. Patterson and R. M. Lambert, Surf. Sci. **187**, 339 (1987).

²J. G. Forbes, A. J. Gellman, J. C. Dunphy, and M. Salmeron, Surf. Sci. **279**, 68 (1992).

³J. Bömermann, M. Huck, J. Kuntze, T. Rauch, S. Speller, and W. Heiland, Surf. Sci. **357/358**, 849 (1996).

⁴T. Rauch, J. Bömermann, P. Borrmann, S. Speller, and W. Heiland, Surf. Sci. **441**, 107 (1999).

⁵F. Maca, M. Scheffler, and W. Berndt, Surf. Sci. **169**, 467 (1985).

⁶M. E. Grillo, C. Stampfl, and W. Berndt, Surf. Sci. **317**, 84 (1994).

⁷W. Liu, K. A. R. Mitchell, and W. Berndt, Surf. Sci. **393**, L119

(1997).

⁸V. R. Dhanak, A. G. Shard, B. C. C. Cowie, and A. Sontoni, Surf. Sci. **410**, 321 (1998).

⁹D. Drakova and G. Doyen, Surf. Sci. **352/354**, 698 (1996).

¹⁰I. S. Tilinin, M. K. Rose, J. C. Dunphy, M. Salmeron, and M. A. van Hove, Surf. Sci. **418**, 511 (1998).

¹¹K. M. Rosso and M. F. Hochella, Jr., Surf. Sci. **423**, 364 (1999).

¹²D. R. Mullins, P. F. Lyman, and S. H. Overbury, Surf. Sci. **277**, 64 (1992).

¹³P. Sautet, J. C. Dunphy, and M. Salmeron, Surf. Sci. **364**, 335 (1996).